

UDC 541.49:546.9:541.6

**A THEORETICAL INVESTIGATION ON THE N—N BOND CLEAVAGE IN Ta(IV)  
HYDRAZIDIUM AND Ta(V) HYDRAZIDO COMPLEXES**

N. Lu<sup>1</sup>, H. Wang<sup>2</sup>

<sup>1</sup>*College of Chemistry and Material Science, Shandong Agricultural University, Taian City, Shandong Prov., P.R. China*

E-mail: lun@sdau.edu.cn

<sup>2</sup>*College of Forestry, Shandong Agricultural University, Taian City, Shandong Prov., P.R. China*

Received December, 15, 2014

Revised — February, 25, 2015

The reaction mechanism of the N—N bond cleavage in Ta(IV) hydrazido and hydrazidium complexes is studied using density functional theory. The N—N bond cleavage in Ta(IV) hydrazidium generates formal Ta(IV) nitridyl. The N—N bond cleavage in Ta(V) hydrazido gives terminal Ta(V) nitrido species. In the tetrahydrofuran solvent, terminal Ta(V) nitrido dimerizes through a one-step direct pathway leading to the [Ta(V),Ta(V)] bis( $\mu$ -nitrido) product. Two Ta—N bonds form simultaneously between the Ta center of one molecule and the terminal N atom of another. In the toluene solvent, there are two pathways of H atom abstraction and protonation producing mononuclear Ta(V) parent imide. The former consists of three steps originated from formal Ta(IV) nitridyl. The latter is unfavorable with terminal Ta(V) nitrido as the precursor.

DOI: 10.15372/JSC20160106

**Key words:** N—N bond cleavage, H atom abstraction, dimerization, protonation, density functional calculation.

## INTRODUCTION

Nitrogen is known to be essential for life. Since the dissociation of the N≡N triple bond is extremely energy intensive, chemists have long searched for the development of efficient transition metal complexes [ 1 ] to mediate the low-energy process in a catalytic cycle such as the "Schrock cycle" [ 2, 3 ]. The Mo(III) complexes were used by Schrock to realize the key N—N bond cleavage. Recently, Odom achieved the conversion of hydrazido(1-) to nitrido catalyzed by Mo(IV) and established possible mechanisms [ 4 ].

The charming Schrock cycle has initiated more and more efforts devoted to the development of other transition metals. A breakthrough of group 4 metals was Shima's dinitrogen cleavage by a tri-nuclear Ti polyhydride complex [ 5 ]. Among viable solutions to the problem of N<sub>2</sub> activation [ 6 ], the better protocol was found when N<sub>2</sub> was bound to two or more metal centers [ 7 ]. Apart from the first complex with coordinated dinitrogen [Ru(NH<sub>3</sub>)<sub>5</sub>N<sub>2</sub>]<sup>2+</sup>, more achievements have been made about group 8 metals, especially in the aspects of Fe. Holland reported the cooperativity between low-valent Fe and K promoters in N<sub>2</sub> activation [ 8 ]. Kuwata obtained the N—N bond cleavage of hydrazines assisted by bifunctional Fe complexes with a pincer-type ligand [ 9 ]. As a comparison, the studies of group 5 metal hydrazides remain relatively scarce. Gray has described Nb and Ta terminal hydrazido(2-) complexes in ligand- and metal-based redox chemistry [ 10 ].

A recent progress has been an improved Schrock cycle of Sita's group [11]. Based on a large number of preliminary experimental works [12], Sita et al. synthesized Ta(IV,  $d^1$ ) hydrazido and hydrazidium complexes supported by the cyclopentadienyl ( $\eta^5\text{-C}_5\text{R}_5$ )/guanidinate ( $\eta^2\text{-}[\text{N}(\text{R}')\text{C}(\text{R}'')\text{N}(\text{R}''')]$ ) (**CpG**) ligand environment [11]. To the best of our knowledge, apart from the calculations on the N—N bond breaking promoted by  $([\text{ArNC(CH}_3)_2\text{CH}]\text{V(ODiiP})$  and  $\text{Mo(N}_2\text{)(HIPTN)}_3\text{N}$  [13], there is no report about the mechanistic study at present. How does the chemical reduction of the Ta(IV) hydrazidium complex generate a  $[\text{Ta(V),Ta(V)}]$  bis( $\mu$ -nitrido) product? Whether it is mononuclear Ta(V) parent imide produced via the protonation of the Ta(V) imide anion or via H atom abstraction from the Ta(IV) nitridyl cation? What is the relationship between the level of  $\text{N}_2$  activation and the transition metal? To resolve these puzzled questions in experiment, we perform a computational study based on density functional theory (DFT). The important elementary steps, intermediates, and transition states are displayed in detail. We hope this work presents an intrinsic mechanism of catalytic group 5 metal variants for further experiments.

### COMPUTATIONAL DETAILS

The DFT calculations were performed using the Gaussian 09 package [14]. To clarify different singlet and doublet states, the B3LYP and UB3LYP approaches, which include Becke's three-parameter hybrid functional combined with the Lee—Yang—Parr correction for correlation [15—17] were used for diamagnetic Ta(V) and paramagnetic Ta(IV) species, respectively. Geometries were optimized with **BSI** basis sets (LanL2DZ with ECP for Ta, 6-31G( $d,p$ ) for the others) [18, 19]. Frequencies were analyzed at the same level to characterize the nature of stationary points (energy minima or first order saddle points) and to provide thermodynamic quantities. The intrinsic reaction coordinate (IRC) paths were also traced to verify the profiles that connect each transition state to the correct associated local minima. Scan calculations were carried out at B3LYP/**BSI** level for important steps.

The solvent effect was calculated using the self-consistent reaction field (SCRF) method [20, 21] based on the integral equation formalism polarizable continuum model (IEFPCM) [22] at the B3LYP/[TZVP+6-311++G( $d,p$ )] level of theory [23, 24]. The energies showed in the whole text were all calculated at this level. For all cited energies, ZPE corrections were taken into consideration.

### RESULTS AND DISCUSSION

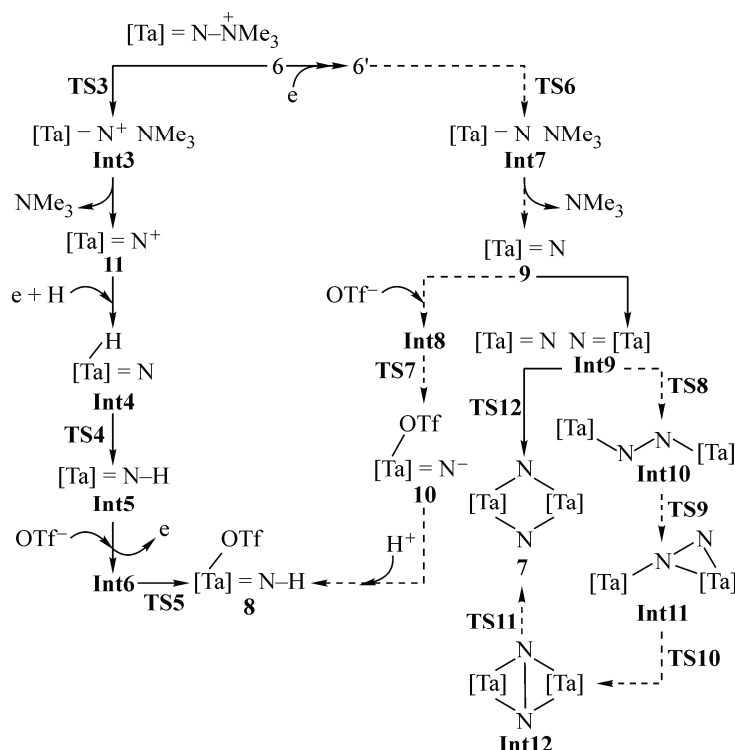
The proposed mechanism is outlined for the N—N bond cleavage in Ta(IV) hydrazidium complex **6** and Ta(V) hydrazido complex **6'** with a simplified **Cp**( $\eta^5\text{-C}_5\text{H}_5$ ) ligand in Scheme 1. Since there are only weak H bonds between the triflate counter anion ( $\text{OTf}^-$ ) and **6**, the omission of  $\text{OTf}^-$  has little effect on the optimized structure of **6**. Thus, in the analysis of pathways, **6** is treated as a cation without  $\text{OTf}^-$ . The energies for all stationary points are calculated relative to the total energy of isolated substrates. The reaction occurs in pentane (C5) and tetrahydrofuran (THF) solvents in the experiment. Thus, the Gibbs free energies in the solution phase are mainly discussed in this paper. In Scheme 2, the relative energy profiles of all pathways in the solvent are depicted in lines of different colors.

**Dimerization pathway.** Seen from Scheme 1, the addition of an electron to cation **6** gives neutral **6'**. The electron affinity is  $-44.3 \text{ kcal}\cdot\text{mol}^{-1}$  in THF solvent. To investigate the important step of the N—N bond breaking more accurately, the Scan calculation was employed along the N1—N2 bond of **6'**. Based on the results, we located the transition state **TS6** corresponding to the cleavage of the N1—N2 bond (1.72 Å). An intermediate of terminal Ta(V) nitrido species **9** was optimized with helpful IRC paths. The energy barrier of this step is  $13.7 \text{ kcal}\cdot\text{mol}^{-1}$  with respect to **6'** (Table 1). The dissociation energy is about  $-49.0 \text{ kcal}\cdot\text{mol}^{-1}$ . The exothermic energy is sufficiently high to facilitate the concentration of **9** in THF, thus providing the opportunity of dimerization. There are two isomers of final product  $[\text{Ta(V),Ta(V)}]$  bis( $\mu$ -nitrido) **7**. The pathways leading to *trans*-**7** were selected to illustrate the detailed reaction mechanism. The Gibbs free energy profiles are depicted in Scheme 2, *a*. The optimized structures of species are displayed in Fig. 1 with key atoms numbered.

Table 1

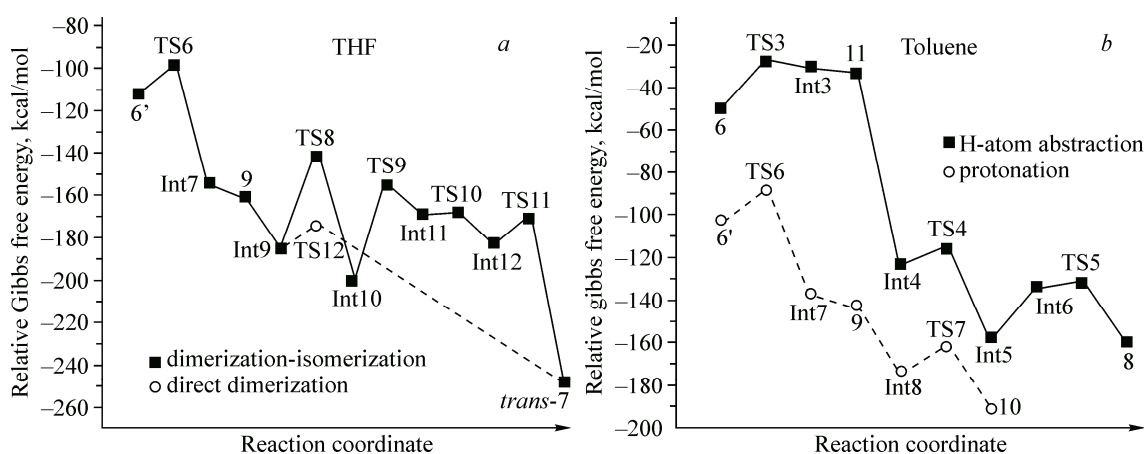
*The Gibbs free energy barrier  
(in kcal·mol<sup>-1</sup>) of all reactions in the gas  
and solution phase calculated with  
B3LYP/6-311++G(d,p)//B3LYP/6-  
31G(d,p) method*

State	$\Delta G^\ddagger$	
	Gas	In solution
<b>TS3</b>	27.9	21.6(toluene)
<b>TS4</b>	9.0	7.5(toluene)
<b>TS5</b>	5.8	1.7(toluene)
<b>TS6</b>	12.9	14.2(toluene) 13.7(THF)
<b>TS7</b>	6.8	11.5(toluene)
<b>TS8</b>	30.9	43.6(THF)
<b>TS9</b>	47.0	45.0(THF)
<b>TS10</b>	2.3	0.4(THF)
<b>TS11</b>	13.2	11.7(THF)
<b>TS12</b>	-19.6	11.0(THF)



Scheme 1. Proposed reaction mechanism for the N—N bond cleavage of Ta(IV) hydrazido and hydrazidium complexes. [Ta] denotes Ta complex supported by **CpG** ligand environment. Different pathways are denoted by green, cyan and dashed line respectively

Bimolecular Ta(V) nitrido complex **Int9** is located with weak H bonds stabilizing the structure. The N1—N3 bond forms (1.93 Å) via transition state **TS8** with a barrier of 43.6 kcal·mol<sup>-1</sup> in step 1. In resultant intermediate **Int10**, the length of the strong N1—N3 bond is 1.29 Å. Then the Ta1—N1—N3—Ta2 structure is twisted to make one Ta center close to non-bonded N. The transition vector of **TS9** corresponds to the approaching of Ta1 to N3 (2.41 Å). The barrier of step 2 is 45.0 kcal·mol<sup>-1</sup> with respect to **Int10**. The formed Ta1—N3 bond is 2.08 Å in **Int11**. At step 3, the structure continues folding to realize the formation of another Ta2—N1 bond via **TS10** (2.85 Å). At this point, the



Scheme 2. Relative Gibbs free energy profile for pathways (a) leading to [Ta(V),Ta(V)] bis( $\mu$ -nitrido) product 7 (b) leading to mononuclear Ta(V) parent imide 8

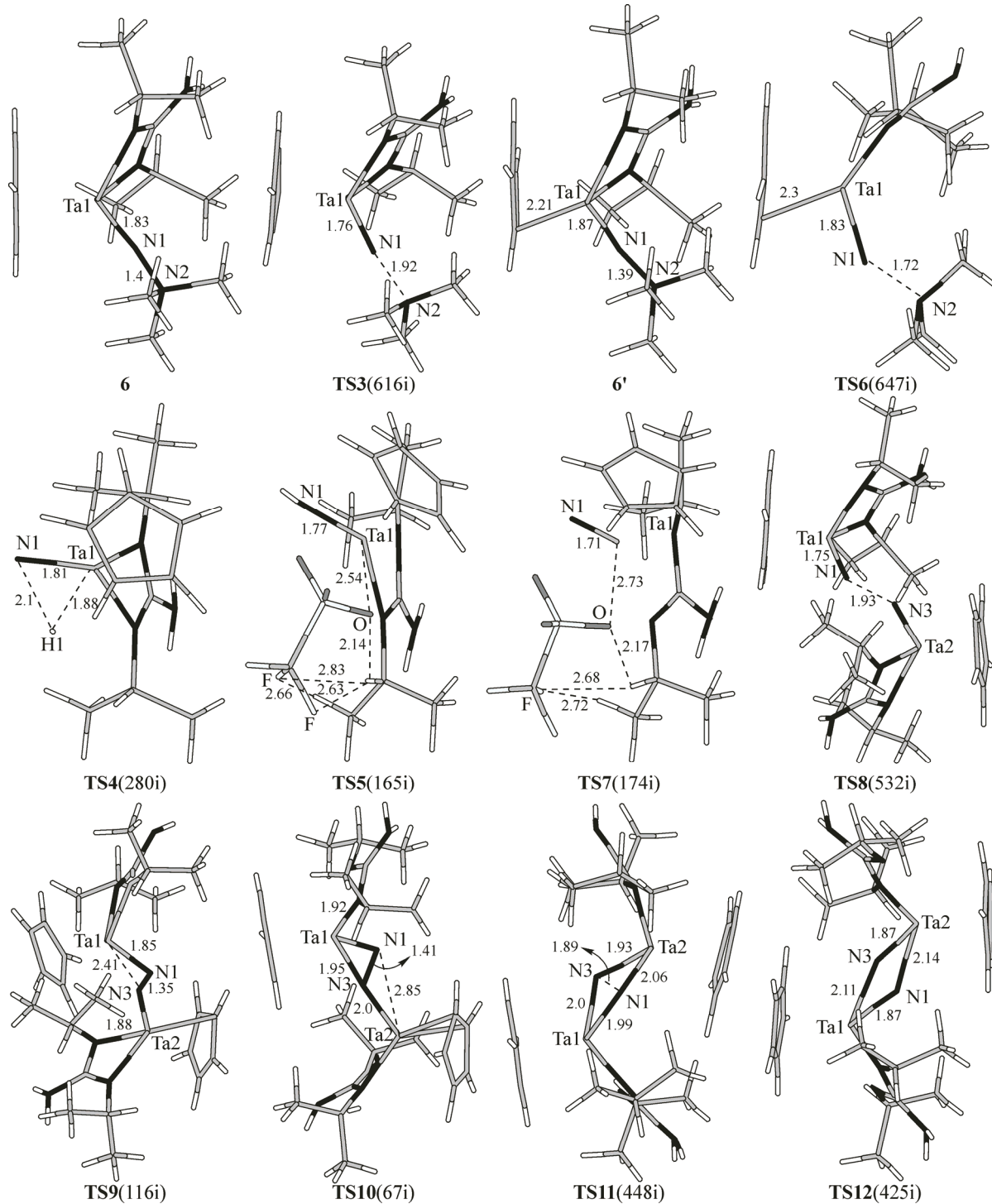


*Fig. 1.* Optimized structure of Ta(IV) hydrazidium **6**, Ta(V) hydrazido **6'** complexes and **TS** in different pathways. The imaginary frequency ( $\text{cm}^{-1}$ ) of **TS** is in parentheses. Bond lengths are in angstroms

N1—N3 bond is stretched to 1.46 Å. In **Int12**, the N—N bond is preliminarily activated. Step 3 is readily accessible with a small barrier of 0.4  $\text{kcal}\cdot\text{mol}^{-1}$  in the THF solvent. Therefore the N<sub>2</sub> activation is continued at the next step, namely the isomerization of **Int12**. At step 4, the N1—N3 bond is cleaved via **TS11** (1.89 Å) with a barrier of 11.7  $\text{kcal}\cdot\text{mol}^{-1}$ . Finally, the stable *trans*-**7** product is obtained with the N1···N3 separation of 2.6 Å and a contracted Ta1···Ta2 distance (2.82 Å).

Although this mechanism is similar to the case suggested by Musaev [25], the barriers of two initial steps are high, which seems to be contradictory with the short reaction time of the experiment [11]. Therefore we assume that a simple path exists along with this complicated mechanism. A transition state **TS12** was successfully located between **Int9** and *trans*-**7** corresponding to the direct dimerization of the mononuclear nitridyl complex. This is the synchronous shortening of Ta1···N3 (2.11 Å) and Ta2···N1 (2.14 Å) distances. As compared with **Int9**, the Ta1—N1 and Ta2—N3 bond lengths are longer (1.87 Å), yet with a small contribution to the transition vector of **TS12**. The correct connection was verified by the IRC path. The barrier of this direct mode is calculated to be 11.0 kcal·mol<sup>-1</sup> in THF. It is undoubtedly determined to be the superior path of dimerization. The direct dimerization mechanism matches the faster generation of **7** in THF solvent of the experiment. Moreover, the exothermic energy is large enough (-60.3 kcal·mol<sup>-1</sup>) to thermodynamically pull the whole reaction. This is also in agreement with the high yield of **7** in the experiment [11].

**H atom abstraction pathway.** In the experiment, another product of the N—N bond cleavage was mononuclear Ta(V) parent imide **8** [11]. We located the H atom abstraction and protonation in two possible pathways originated from hydrazidium **6** and hydrazido **6'**, respectively. The relative Gibbs free energy profiles are shown in Scheme 2, *b*.

We discuss the former at first. In the same way, the transition state **TS3** was obtained by virtue of Scan calculations along the N1—N2 bond of **6**. The N1—N2 bond dissociation proceeds via **TS3** (1.92 Å) with a barrier of 21.6 kcal·mol<sup>-1</sup> in the toluene solvent. From the comparison of resulting formal Ta(IV) nitridyl species **11** with **6** it follows that the energy of 16.1 kcal·mol<sup>-1</sup> is required for step 1 to break the N1—N2 bond. As one H atom and one electron are supplied to **11**, uncharged Ta(IV) hydride intermediate **Int4** is located with a newly formed Ta1—H1 bond (1.76 Å). Under the effect of electron affinity, the negative hydrogen ion greatly stabilizes cation **11**. As a result, the energy of **Int4** is 73.7 kcal·mol<sup>-1</sup> lower than that of **6**. Successively at step 2, H1 is attracted by the terminal N1 atom from the Ta1 center via **TS4** with a low barrier of 7.5 kcal·mol<sup>-1</sup>. The atomic motion has been described during the elongation of the Ta1—H1 bond (1.88 Å) and the shrinkage of the N1—H1 bond (2.10 Å) in **TS4**. This generates more stable Ta(IV) imide intermediate **Int5**. At step 3, **Int5** is attacked by additional OTf<sup>-</sup> and one electron is taken away. Hence, neutral Ta(V) pre-complex **Int6** is acquired, the structure of which is supported by multiple H bonds between F, O of OTf<sup>-</sup>, and C—H of the **G** ligand. The approach of OTf<sup>-</sup> to the Ta center goes through **TS5** with the formation of the Ta1—O bond (2.54 Å). In Ta(V) parent imide **8**, the Ta1—O bond is completely formed (2.1 Å). Step 3 is exothermic (-26.2 kcal·mol<sup>-1</sup>) and demands the activation energy of only 1.7 kcal·mol<sup>-1</sup>.

**Protonation pathway.** The alternative protonation pathway takes neutral Ta(V) **6'** as the precursor. Step 1 involves the production of **9** via **TS6** just like in the case mentioned in the dimerization pathway. The difference is in the solvent. The energy barrier of step 1 is 14.2 kcal·mol<sup>-1</sup> in toluene and the dissociation energy is -39.6 kcal·mol<sup>-1</sup>. At step 2, with available OTf<sup>-</sup>, **9** can also form monovalent negatively charged Ta(V) intermediate **Int8** stabilized by multiple H bonds. It is noted that the energy of **Int8** is 16.9 kcal·mol<sup>-1</sup> lower than that of structurally similar **Int6** in the gas phase. The discrepancy is enlarged by 23.0 kcal·mol<sup>-1</sup> in toluene. This is presumably because the stabilizing effect of the solvent on the **Int8** anion is better than that on the neutral **Int6** molecule [26]. A transition state **TS7** corresponding to the approach of O to Ta1 (2.73 Å) is located with a barrier of 11.5 kcal·mol<sup>-1</sup>. The Ta1—O bond is formed (2.17 Å) in Ta(V) imide anion **10**. The energy is decreased by 17.9 kcal·mol<sup>-1</sup> as compared to that of **Int8**. Since the ion binding reaction is extremely easy, **10** is protonated with the formation of **8** with an adventitious proton. However, step 2 is endothermic (13.7 kcal·mol<sup>-1</sup>). With regard to that **8** is less stable than **10**, we anticipate this pathway to be unfavorable.

## CONCLUSIONS

In conclusion, a detailed mechanism for the N—N bond cleavage in Ta(IV) hydrazido and hydrazidium complexes for N<sub>2</sub> activation has been systematically investigated by performing DFT calculations. The calculated results indicate that the N—N bond cleavage in Ta(IV) hydrazidium generates

formal Ta(IV) nitridyl. The N—N bond cleavage in Ta(V) hydrazido gives terminal Ta(V) nitrido species. In the THF solvent, terminal Ta(V) nitrido is inclined to dimerize through a one-step direct pathway leading to the [Ta(V),Ta(V)] bis( $\mu$ -nitrido) product. Two Ta—N bonds form simultaneously between the Ta center of one molecule and the terminal N atom of another. Another four-step case is disadvantageous owing to the high barrier of initial steps, despite the feasible isomerization at the last step. In the toluene solvent, there are H atom abstraction and protonation in two pathways for the production of the mononuclear Ta(V) parent imide. The former consists of three steps. After the formation of formal Ta(IV) nitridyl at Step 1, it accepts the H atom and one electron, yielding uncharged Ta(IV) nitridyl hydride at step 2. Step 3 involves the loss of one electron and the combination of OTf<sup>−</sup>. The latter is comprised by two steps with terminal Ta(V) nitrido as the precursor at step 1. Then it is linked to OTf<sup>−</sup> at step 2 and protonated rapidly without any transition state. Thermodynamically, the latter is unfavorable. The present theoretical results not only clearly illuminate the unsolved problems in the experiment but significantly establish a new intrinsic mechanism for Ta hydrazido and hydrazidium complexes.

This work was supported by Natural Science Foundation of Shandong Province (2014ZRB01A3P) and National Natural Science Foundation of China (31070550).

Electronic Supplementary data available: calculated relative energies for the ZPE-corrected Gibbs free energies ( $\Delta G_{\text{gas}}$ ), relative solvation energies ( $\Delta G_{\text{solv}}$ ) and Gibbs free energies ( $\Delta G_{\text{sol}}$ ) for all species in the solution phase at 298 K; Cartesian coordinates for all optimized structures.

#### REFERENCES

1. Hinrichsen S., Broda H., Gradert C. et al. // Annu. Rep. Prog. Chem., Sect. A: Inorg. Chem. – 2012. – **108**. – P. 17 – 47.
2. Yandulov D.V., Schrock R.R. // Science. – 2003. – **301**. – P. 76 – 78.
3. Schrock R.R. // Acc. Chem. Res. – 2005. – **38**. – P. 955 – 962.
4. DiFranco S.A., Staples R.J., Odom A.L. // Dalton Trans. – 2013. – **42**. – P. 2530 – 2539.
5. Shima T., Hu S. W., Luo G. et al. // Science. – 2013. – **340**. – P. 1549 – 1552.
6. Fryzuk M.D. // Science. – 2013. – **340**. – P. 1530 – 1531.
7. Fryzuk M.D. // Chem. Commun. – 2013. – **49**. – P. 4866 – 4868.
8. Figg T.M., Holland P.L., Cundari T.R. // Inorg. Chem. – 2012. – **51**. – P. 7546 – 7550.
9. Umehara K., Kuwata S., Ikariya T. // J. Am. Chem. Soc. – 2013. – **135**. – P. 6754 – 6757.
10. Tonks I.A., Durrell A.C., Gray H.B. et al. // J. Am. Chem. Soc. – 2012. – **134**. – P. 7301 – 7304.
11. Keane A.J., Zavalij P.Y., Sita L.R. // J. Am. Chem. Soc. – 2013. – **135**. – P. 9580 – 9583.
12. (a) Yonke B.L., Reeds J.P., Zavalij P.Y., Sita L.R. // Angew. Chem., Int. Ed. – 2011. – **50**. – P. 2342 – 12346.  
(b) Reeds J.P., Yonke B.L., Zavalij P.Y., Sita L.R. // J. Am. Chem. Soc. – 2011. – **133**. – P. 18602 – 18605.  
(c) Fontaine P.P., Yonke B.L., Zavalij P.Y., Sita L.R. // J. Am. Chem. Soc. – 2010. – **132**. – P. 12273 – 12285.
13. (a) Sgrignani J., Franco D., Magistrato A. // Molecules. – 2011. – **16**. – P. 442 – 465. (b) Tran B.L., Pinter B., Nichols A.J. et al. // J. Am. Chem. Soc. – 2012. – **134**. – P. 13035 – 13045.
14. Frisch M.J. et. al. // Gaussian 09, Revision B.01. – Wallingford, CT: Gaussian Inc., 2009.
15. Becke A.D. // J. Chem. Phys. – 1993. – **98**. – P. 5648 – 5652.
16. Becke A.D. // J. Chem. Phys. – 1996. – **104**. – P. 1040 – 1046.
17. Lee C., Yang W., Parr R.G. // Phys. Rev. B. – 1998. – **37**. – P. 785 – 789.
18. Hay P.J., Wadt W.R. // J. Chem. Phys. – 1985. – **82**. – P. 299 – 310.
19. Wadt W.R., Hay P.J. // J. Chem. Phys. – 1985. – **82**. – P. 284 – 298.
20. Tapia O. // J. Math. Chem. – 1992. – **10**. – P. 139 – 181.
21. Tomasi J., Persico M. // Chem. Rev. – 1994. – **94**. – P. 2027 – 2094.
22. Tomasi J., Mennucci B., Cammi R. // Chem. Rev. – 2005. – **105**. – P. 2999 – 3093.
23. Schaefer A., Huber C., Ahlrichs R. // J. Chem. Phys. – 1994. – **100**. – P. 5829 – 5835.
24. Ide T., Takeuchi D., Osakada K. // Chem. Commun. – 2012. – **48**. – P. 278 – 280.
25. Zhang W., Tang Y., Lei M. et al. // Inorg. Chem. – 2011. – **50**. – P. 9481 – 9490.
26. (a) Lu N., Meng L., Chen D.Z. et al. // J. Phys. Chem. A. – 2012. – **116**. – P. 670 – 679. (b) Lu N., Wang H. // Dalton Trans. – 2013. – **42**. – P. 13931 – 13939.